

# Preliminary design of a tangentially viewing imaging bolometer for NSTX-U

journal or publication title	Review of Scientific Instruments
volume	87
number	11
page range	11D410
year	2016-11-14
URL	<a href="http://hdl.handle.net/10655/00012813">http://hdl.handle.net/10655/00012813</a>

doi: 10.1063/1.4955278



# Preliminary design of a tangentially viewing imaging bolometer for NSTX-U<sup>a)</sup>

B. J. Peterson<sup>1,2,b</sup>, R. Sano<sup>3</sup>, M. L. Reinke<sup>4</sup>, J. M. Canik<sup>4</sup>, L. F. Delgado-Aparicio<sup>5</sup>, J. D. Lore<sup>4</sup>, K. Mukai<sup>1,2</sup>, T. K. Gray<sup>4</sup>, G. G. van Eden<sup>6</sup> and M. A. Jaworski<sup>5</sup>

<sup>1</sup>National Institute for Fusion Science, Toki 509-5292, Japan

<sup>2</sup>SOKENDAI (The Graduate University for Advance Studies), Toki 509-5292, Japan

<sup>3</sup>National Institutes for Quantum and Radiological Science and Technology, Naka, Ibaraki 311-0193, Japan

<sup>4</sup>Oak Ridge National Laboratory, Oak Ridge, Tennessee 37831, USA

<sup>5</sup>Princeton Plasma Physics Laboratory, Princeton, New Jersey 08543, USA

<sup>6</sup>FOM Institute DIFFER, 5612 AJ, Eindhoven, The Netherlands

(Presented XXXXX; received XXXXX; accepted XXXXX; published online XXXXX)

(Dates appearing here are provided by the Editorial Office)

The InfraRed imaging Video Bolometer measures plasma radiated power images using a thin metal foil. Two different designs with a tangential view of NSTX-U are made assuming a 640 x 480 (1280 x 1024) pixel, 30 (105) fps, 50 (20) mK, IR camera imaging the 9 cm x 9 cm x 2 micron Pt foil. The foil is divided into 40 x 40 (64 x 64) IRVB channels. This gives a spatial resolution of 3.4 (2.2) cm on the machine mid-plane. The noise equivalent power density of the IRVB is given as 113 (46)  $\mu\text{W}/\text{cm}^2$  for a time resolution of 33 (20) ms. Synthetic images derived from SOLPS data using the IRVB geometry show peak signal levels ranging from  $\sim 0.8$  -  $\sim 80$  ( $\sim 0.36$  -  $\sim 26$ )  $\text{mW}/\text{cm}^2$ .

## I. Introduction

The InfraRed imaging Video Bolometer (IRVB) measures plasma radiated power images by using a thin foil to absorb the radiation incident on the foil through a small aperture from the plasma. The radiated power absorbed by the thin metal foil is calculated from the change in the foil temperature using the two dimensional (2D) heat diffusion equation of the foil. The temperature of the foil is measured in 2D using an IR camera viewing the side of the foil opposite the plasma through a vacuum IR window from outside the vacuum vessel [1]. Calibration techniques have been developed to determine the spatial variation of the foil thermal parameters ( $\kappa$ , heat diffusivity,  $kt_f$  product of heat conductivity,  $k$ , and foil thickness,  $t_f$ , and  $\epsilon$ , black body emissivity of graphite blackened foil) resulting in an absolutely calibrated instrument [2-4]. In a tokamak, with the assumption of axis-symmetry, a tangentially viewing IRVB can provide numerous lines of sight to be used in a tomographic reconstruction of the 2D radiation profiles [5]. Also radiation images can be directly compared to synthetic images derived from an impurity transport model [6] such as SOLPS [7] or EMC3-Eirene [8,9]. In this paper we give information on the design of an imaging bolometer with a tangential view of NSTX-U [10]. In Section II the IRVB design is described including the choice of the IR camera and the geometry of the bolometer camera. In Section III the sensitivity of the IRVB is quantified through a calculation of the noise equivalent power and the signal is estimated roughly and using synthetic images based on SOLPS data. In Section IV conclusions are drawn and the paper is

summarized.

## II. IRVB DESIGN

The IRVB design consists of (1) the design of the bolometer camera geometry which determines the field of view (FoV) of the IRVB and the number of channels and (2) the choice of the IR camera and the design of the IR optics which are used to bring the IR signal from the foil to the IR camera. In this preliminary design paper the IR optics are neglected and only the FoV is designed.

### A. IR camera parameters

Two different IR cameras are considered in the design of the IRVB. The first is a microbolometer ( $\mu\text{bolo}$ ) detector based IR camera with the parameters 640 x 480 pixels, frame rate of 30 fps and noise equivalent temperature (NET),  $\sigma_{IR}$ , of 50 mK. The second is an InSb detector based IR camera with the parameters 1280 x 1024 pixels, frame rate of 105 fps and NET of 20 mK. Although the InSb detector is faster and more sensitive than the  $\mu\text{bolo}$  detector, it is more expensive and the housing tends to be larger and may require more shielding from the magnetic field if it uses an electromechanical cooler. The InSb detector can also be cooled by liquid Nitrogen, but this requires extra care and handling and a radioactive environment would require remote supplying of the liquid Nitrogen. The  $\mu\text{bolo}$  detectors are usually fitted with an electromechanical shutter for calibration purposes and these also require additional magnetic shielding, but recently, pneumatically driven shutters have been applied to avoid this problem. In the rest of the paper the parameters for the IRVB with the InSb IR camera are shown in parentheses.

<sup>a)</sup>Contributed paper published as part of the Proceedings of the 21st Topical Conference on High-Temperature Plasma Diagnostics, Madison, Wisconsin, June, 2016.

<sup>b)</sup>Author to whom correspondence should be addressed: peterson@LHD.nifs.ac.jp.

## B. Bolometer camera design

Both IR camera cases assume a bolometer camera consisting of a 9 cm x 9 cm Pt foil blackened with graphite with a thickness of 2  $\mu\text{m}$ . The distance from the 2.6 mm x 2.6 mm (1.6 mm x 1.6 mm) aperture (with area,  $A_{ap}$ ) to the foil,  $l_{ap-f}$ , is 58 mm. The IR camera views the foil radially from a mid-plane port, but the square foil is tilted to face the plasma tangentially, giving a rectangular view of the foil that matches the aspect ratio of the field of view (FOV) of the IR camera. This provides a tangential bolometer FoV of the lower hemisphere of approximately half of the torus of NSTX-U without requiring a tangential port. The 8 cm x 8 cm central section of the foil is divided into 40 x 40 (64 x 64) IRVB channels, each consisting of 141 (220) IR camera pixels. This gives a spatial resolution of 3.4 cm (2.2 cm) on the mid-plane at the plane of tangency to the central viewing chord. A top view of NSTX-U with the foil and aperture locations and the edges of the field of view is shown in Figure 1. The computer aided drawing (CAD) of the FoV for the  $\mu\text{bolo}$  case is shown in Figure 2. The FoV for the InSb case is the same except that the number of channels is increased. The top row of channels is centered on the machine mid-plane with the lower rows looking down into the lower divertor. The left hand column of channels views directly into the machine in the major radial direction with the subsequent columns fanning out tangentially.

## III. SIGNAL to NOISE ESTIMATION

### A. Noise equivalent power estimates

The noise equivalent power (NEP),  $\eta_{IRVB}$ , is a figure of merit for the IRVB sensitivity and is derived as Equation 10 in reference [1] by propagating the error in the temperature measurement by the IR camera (NET) through the 2D heat diffusion equation of the foil solved for the radiated power. The noise equivalent power density (NEPD),  $S_{IRVB}$ , is given in Equation 1

$$S_{IRVB} = \frac{\eta_{IRVB} N_{bol}}{A_f} = \frac{\sqrt{10kt_f \sigma_{IR}}}{\sqrt{f_{IR} N_{IR}}} \sqrt{\frac{N_{bol}^3 f_{bol}^3}{A_f^2} + \frac{N_{bol} f_{bol}^3}{5\kappa^2}} \quad (1)$$

with  $N_{bol}$ , number of bolometer channels,  $A_f$ , utilized area of the

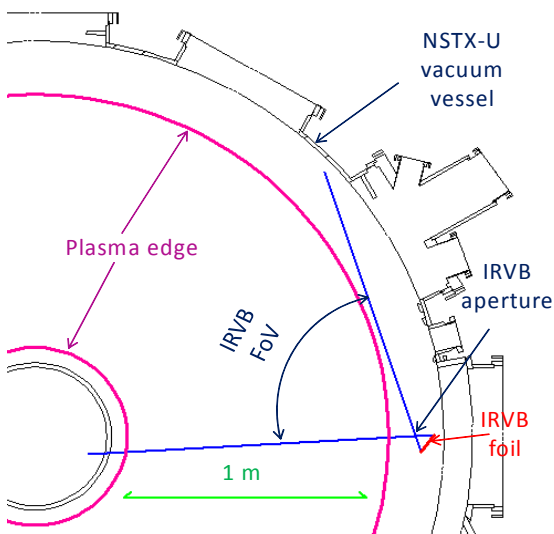


FIG. 1. CAD of top view of NSTX-U midplane showing foil and aperture locations and FoV of IRVB.

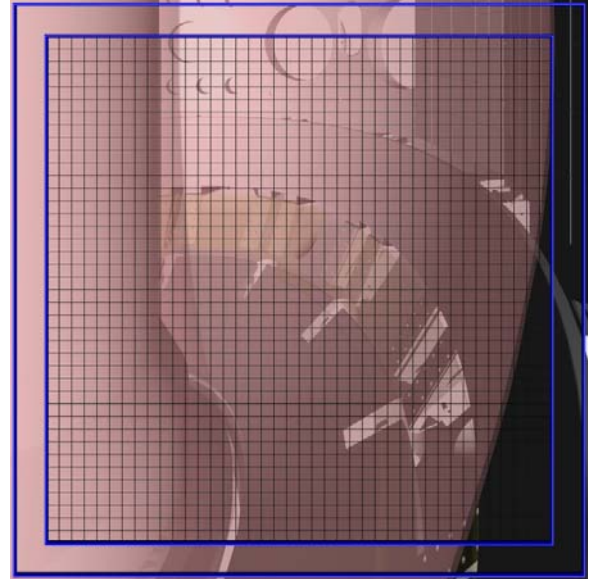


FIG. 2. CAD of FoV of IRVB with tangential view of NSTX-U for  $\mu\text{bolo}$  case with 40 x 40 channels indicated by the gray grid. The plasma is indicated by pink and the blue border lines indicate the 9 cm x 9 cm edge of the foil and the 8 cm x 8 cm edge of the usable portion of the foil.

foil,  $f_{IR}$ , frame rate of IR camera,  $f_{bol}$ , effective frame rate of bolometer,  $N_{IR}$ , utilized number of IR camera pixels. Equation 1 is derived from the above mentioned NEP expression by neglecting the black body radiation term (third term under the radical) and dividing by the bolometer pixel area ( $A_{bol} = A_f/N_{bol}$ ). Using this expression the NEPD of the IRVB is given as 113  $\mu\text{W}/\text{cm}^2$  ( $46 \mu\text{W}/\text{cm}^2$ ) for a time resolution of 33 ms (limited by the IR camera frame rate) (20 ms).

### B. Signal estimates

A rough estimation of the radiated power density at the foil,  $S_{signal}$ , is given by Equation 2

$$S_{signal} = \frac{P_{signal}}{A_{bol}} = \frac{A_{bol} A_{ap} \cos^4 \theta P_{rad} l_{plasma}}{A_{bol} 4\pi^2 l_{ap-f}^2 V_{plasma}} \quad (2)$$

where  $\theta = 20^\circ$  is the average angle between the sight line and the foil normal vector.  $P_{rad} = 2 \text{ MW}$  of radiated power is assumed to be uniformly emanating from the  $V_{plasma} = 11 \text{ m}^3$  volume plasma. The signal level is therefore estimated to be  $5.7 \text{ mW}/\text{cm}^2$  ( $2.2 \text{ mW}/\text{cm}^2$ ). Taking the ratio of Equation 2 divided by Equation 1 gives a signal to noise ratio (SNR) of 51 (48).

### C. Synthetic images

Synthetic images are derived from 2D SOLPS (version 5.0) carbon and deuterium radiation data by assuming toroidal symmetry and integrating the data along the lines of sight of the viewing chords of each IRVB detector. Three SOLPS cases are considered having input power of 10 MW and core densities of 2, 5 and  $10 \times 10^{19}/\text{m}^3$ , respectively. Peak signal levels ranging from  $\sim 0.8$  -  $\sim 80 \text{ mW}/\text{cm}^2$  ( $\sim 0.36$  -  $\sim 26 \text{ mW}/\text{cm}^2$ ) depending on the plasma density.

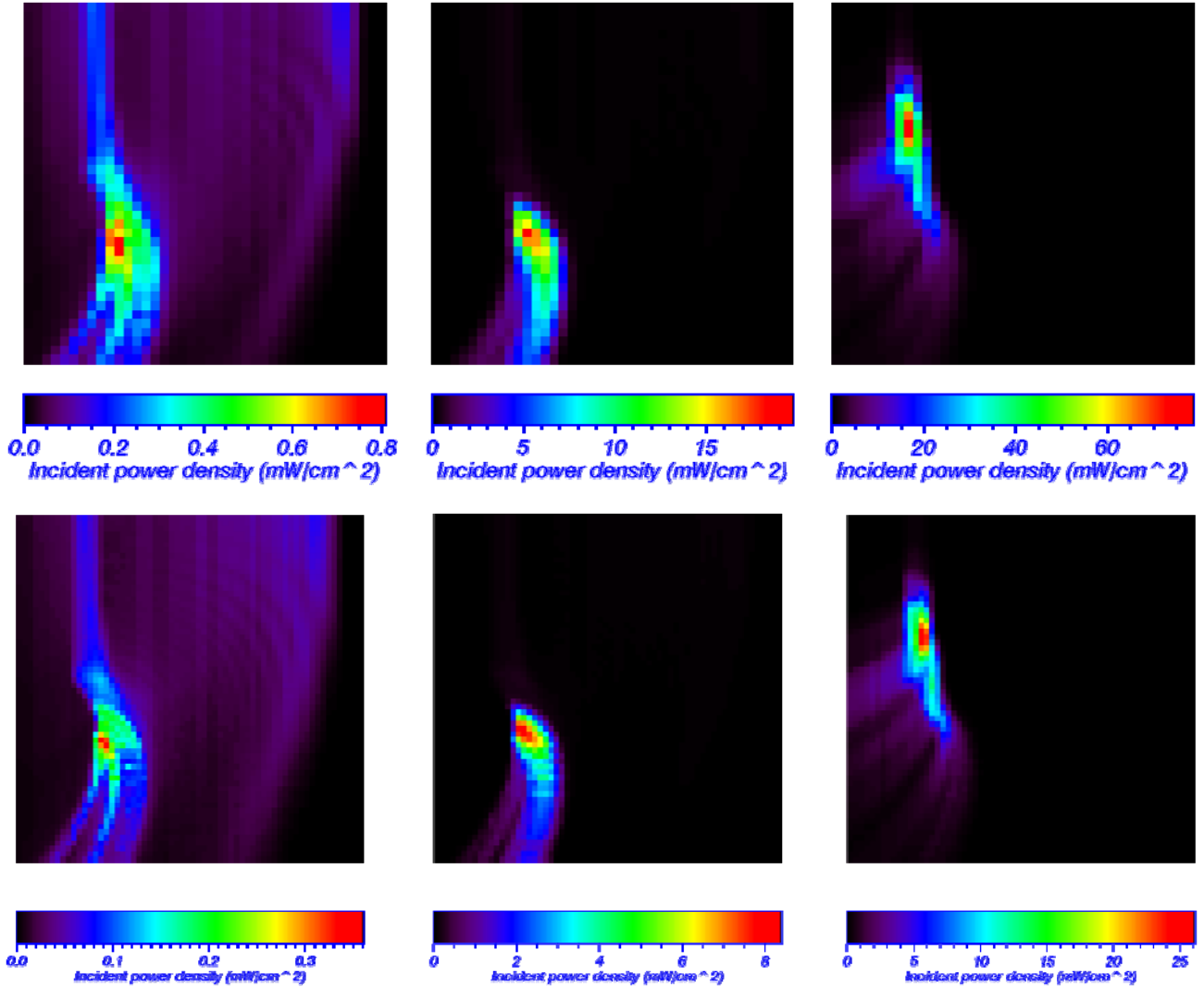


FIG. 3. Synthetic images for carbon and deuterium radiation from SOLPS data for the  $\mu$ bolo (upper row,  $N_{bol} = 40 \times 40$ ) and InSb (lower row,  $N_{bol} = 64 \times 64$ ) cases for core densities of 2 (left), 5 (center) and 10 (right)  $\times 10^{19}/\text{m}^3$ .

#### IV. CONCLUSIONS

These synthetic images demonstrate that the IRVB has sufficient sensitivity and spatial resolution to resolve changes in the radiation structure with density as predicted by SOLPS. The advantage of the larger number of pixels and the higher sensitivity of the InSb detector in resolving the details of the divertor radiation is evident in the comparison with the  $\mu$ bolo case. The 1.5 times improvement in spatial resolution for the InSb case is a result of the 2.64 times smaller aperture area, which corresponds to the reduction in signal according to Eq. 2. However, since the IRVB NEPD of the InSb case is also 2.45 times smaller, the InSb case SNR is only slightly smaller. In addition, the InSb case has 1.65 times the temporal resolution of the  $\mu$ bolo case. In further design work tradeoffs can be made between SNR, spatial and temporal (down to the hard limit of the IR camera frame time) resolutions to optimize the IRVB for the experimental conditions.

#### V. ACKNOWLEDGMENTS

The authors acknowledge the support of the NSTX-U team and from the National Institute for Fusion Science (Japan) budget NIFS15ULHH026 and the Department of Energy (USA) contract numbers DE-AC05-00OR22725 and DE-AC02-09CH11466. One of the authors (B.J.P.) would also like to thank the Department of Energy (USA) and the National Institutes for Natural Sciences (JAPAN) for financial support during his sabbatical visit to Princeton Plasma Physics Laboratory in 2015.

<sup>1</sup>B. J. Peterson et al., Rev. Sci. Instrum. **74** (2003) 2040.

<sup>2</sup>R. Sano et al., Plasma Fusion Res. **7** (2012) 2405039.

<sup>3</sup>S.N. Pandya et al. Rev. Sci. Instrum. **85** (2014) 054902.

<sup>4</sup>K. Mukai et al., Rev. Sci. Instrum. **85** (2014) 11E435.

<sup>5</sup>B. J. Peterson et al., Plasma Fusion Res. **2** (2007) S1018.

<sup>6</sup>B. J. Peterson et al., J. Nucl. Mater. **415** (2011) S1147.

<sup>7</sup>D. P. Coster et al., Phys. Scr. **T104** (2004) 7.

<sup>8</sup>Y. Feng et al., Contrib. Plasma Phys. **44** (2004) 57.

<sup>9</sup>D. Reiter et al., Fusion Sci. Technol. **47** (2005) 172.

<sup>10</sup>M. Ono et al., Nucl. Fusion **55** (2015) 073007.